

USE OF LIMIT ANALYSIS METHODS TO ASSESS THE STRUCTURAL CAPACITY OF SUBSEA SYSTEMS AND COMPONENTS

Chris Alexander
Stress Engineering Services, Inc.
Houston, Texas
chris.alexander@stress.com

ABSTRACT

With advances in computational modeling techniques, limit load methods are gaining wider acceptance as a tool for determining the integrity of structural and pressure containing systems. The objective of a limit load analysis is to size a vessel or structure considering nonlinearities such as elastic-plastic material properties and non-linear strain-displacement relations. It is even possible to use experimental methods to determine the loading capacity of a structure [1]. In subsea and offshore environments, there are a variety of conditions that can lead to the need for limit analyses.

Case studies are presented in this paper that feature scenarios including external pressures, pipe axial tension and bending, and dropped object impact loads. The limit load technique applies an appropriate initial magnitude for each load type and uses an analysis model or test set-up to increase the load until a lower bound load is calculated. The lower bound value is determined by incrementally increasing the load until the structures can no longer support additional loading without gross plastic deformation.

This paper presents how limit load techniques were used to address the structural integrity of four engineered systems. These include the design of a subsea vessel under elevated external pressures, assessing the remaining buckling resistance of a dented subsea flowline, determining the effects of impact loads on an export riser, and evaluating the ability of a composite repair to reinforce a corroded riser using experimental methods.

SUBSEA ELECTRONIC HOUSING

A manufacturer of electronic equipment for subsea applications needed to optimize a design to achieve maximum water depths. Using a conceptual design, several analyses were performed using limit load methods. The primary design considerations involved geometric requirements associated with battery sizes and a design depth of 3,000 meters (9,840 feet). Initial efforts to size the dimensions of the design involved the use of a finite element model with shell elements. Once the geometry for the design was finalized, a limit analysis was performed using a model with solid eight-node hexagonal elements. The final analysis results demonstrated that the final geometry was adequately designed for the 3,000 meter depth requirement. Additionally, full-scale testing involving an external pressure of 10,000 psi proved the adequacy of the design. The sections that follow are some of the details on the analysis methods and results.

Preliminary Shell Model

Initial work involved using classical mechanics equations for basic sizing purposes. Once overall dimensions were determined, a preliminary finite element model using shell elements was constructed.

In a design process, the shell element has an advantage in that its local thickness can be modified as an input variable, whereas solid elements require a complete reconstruction of the model geometry whenever dimensions such as wall thicknesses are changed. **Figure 1** is a view of the basic shell finite element model.

Using the shell element model, wall thicknesses were determined for specific regions of the subsea housing that could meet both the geometric and operating requirements of the design criteria. The results of this portion of the analysis determined the geometry for the final design. The final analysis involved the construction of a solid model that included the main body of the housing, the lid, simulated bolting, and contact interaction between the lid and body.

Both the shell and solid models used limit load analysis. Elastic perfectly-plastic material properties for the aluminum 7075 material were input into the finite element model and external pressure was ramped up until convergence of the model was no longer possible. Because the primary intent of this project was development of a final design, the sections that follow provide specific details on the methods and results associated with the analysis of the solid element model.

Solid Model Analysis

The analysis of the three-dimensional finite element model using solid elements involved the following details:

- Geometry included the outer cylinder of the main body housing, internal ribs oriented radially outward, 0.85-inch thick internal plate, and a 0.90-inch thick lid.
- Contact was modeled between the lid and the main body housing. Contact was generated on top of the ribs and in the recessed portion on each end of the housing.
- Bolting to attach the lid to the housing was accomplished by connecting nodes on the lid and body. This connection method was used for eight (8) regions on the housing located 45 degrees apart circumferentially.
- A symmetry plane was invoked half-way between the ends of the housing. This cut the 0.85-inch internal plate in half. As with the shell model, this boundary condition prevents nodes on the symmetry plane from displacing in the 3-direction and prevents rotations about the 1-direction and 2-direction.
- External pressure was of 10,000 psi was applied to all outside surfaces of the housing model including the lid and the cylinder. This value that exceeds that design requirement of 3,000 meters (approximately 4,370 psi), but was thought to be high enough that convergence would be unlikely for the current design.

As with the shell models, the lower bound limit load was obtained by increasing external pressure on the finite element model to the point where the structure fails to withstand any additional load (i.e. convergence of the finite element solution was no longer possible).

Figure 2 provides an isometric view of the solid finite element model that includes details on the boundary conditions.

When ABAQUS solves a finite element problem, it produces a status file (e.g. *model_input.sta*) that reports the convergence parameters for the respective model. When performing a limit analysis, information contained within this file is useful. Provided in **Figure 3** is the output data obtained for the solid finite element model. In this figure two columns are important.

- The data plotted in **RED** constitute an increment fraction of applied load. A value of 0.10 implies that 10 percent of the total load has been applied. The model stopped when an increment fraction of 0.941 was reached. For the problem at hand this means that the lower bound limit load is 94.1 percent of the total applied load (i.e. 10,000 psi). Consequently, the calculated lower bound limit load is 9,410 psi that corresponds to a subsea depth of 6,461 meters. To this value a design safety factor is applied.
- The data plotted in **BLUE** constitute deflection of a tied node where a bolt was assumed to exist. Although not necessarily applicable for the problem at hand, deflection data is often useful for creating load-deflection plots. At the end of the load step, disproportionately large deflections of the structure take place with small increases in load.

Having calculated the lower bound limit load, it is appropriate to discuss the design criterion that determined the allowable safe operating depth for the subsea housing. The calculated lower bound limit load is 9,410 psi (as shown in **Figure 3**), or 6,461 meters. Division 3 of the ASME Boiler & Pressure Vessel Code permits a factor of 2.0 on the lower bound limit load without restrictions (since the time during which this analysis was completed, the design margin has changed such that the current factor is 1.732. The phrase *without restrictions* is a reference to Division 2 that permits a 1.5 factor but requires wall thickness be not less than the classical equations allow). Using this design factor, a design pressure of 4,704 psi is calculated that corresponds to a sea depth of 3,230 meters. This design depth value exceeds the minimum design requirement of 3,000 meters. This design pressure is conservative and thought to satisfy the prescribed design requirements for the subsea housing, which was validated by experimental work that demonstrated the design was good for more than 7,000 psi. The only observed anomaly after testing was deformation of the internal ribs resulted in a plastic deformation of 0.025 inches. There was no plastic deformation of the lid covering.

Figure 4 shows the deformation of the main body of the subsea housing from the solid finite element analysis with an external pressure of 9,410 psi. Note in this figure the deformation of the internal rib structure, which is consistent with the conditions observed experimentally in the external pressure testing.

SUBSEA DENTED PIPELINE

A subsea pipeline in the Gulf of Mexico was impacted by a ship anchor. This impact resulted in generating a longitudinally-oriented dent in the pipeline. Inspections revealed that no cracks were presented; however, concerns existed about the effects of the dent on the mechanical integrity of the pipeline. The line was fabricated from Grade X70 pipe having a diameter of 8.625 inches and a wall thickness of 0.656 inches. The dent had an estimated profile of 0.72 inches deep with a length of 13.8 inches based upon measurements scaled from

photos taken subsea. The pipeline operates at a maximum allowable operating pressure (MAOP) of 7,700 psia and is located at a water depth of 7,150 feet.

Due to the thick wall of the pipe, solid three-dimensional elements were required. ABAQUS was used to process and post-process the analysis results. Elastic-plastic material properties based on an actual stress-strain curve along with nonlinear options for geometric displacements were used.

Finite element modeling was employed to assess the effects of the dent on the structural integrity of the pipeline. While some portion of this effort involved fatigue assessment due to cyclic pressures, the focus of the data for this paper is collapse due to external pressure. In deepwater applications, considerations require that external pressure be considered as a design load. In most subsea pipeline applications, the potential for collapse due to external pressure governs design, especially with regards to the required wall thickness. When deepwater subsea pipelines are permanently damaged in a manner that changes the ovality of the pipe, evaluation is required to determine the effect on the buckling capacity of the pipeline. The finite element analysis involved the following load steps.

- Step #1: Apply internal pressure to the inside of the pipe (4,525 psi - difference between MAOP and external pressure of 3,175 psi corresponding to 7,150 feet of sea water)
- Step #2: Move indenter to make contact with pipe
- Step #3: Push indenter into pipe to a depth of 1.0 inches
- Step #4: Remove indenter and determine residual dent depth (found to be 0.786 inches)
- Step #5: Remove internal pressure
- Step #6: Apply an internal pressure of 4,525 psi
- Step #7: Remove internal pressure (0 psi differential between inside and outside of pipe)
- Step #8: Apply external pressure of 12,700 psi to outside of sample (perform a limit analysis to determine buckling capacity of flowline considering the presence of a dent)

Steps #6 and #7 represent the extremes of a full pressure cycle. Stresses extracted from these load steps were used to calculate the stress range used in the fatigue analysis. Using the fatigue methods outlined in Appendix 5 of the ASME Boiler & Pressure Vessel Code, Section VIII, Divisions 2, the design fatigue life was calculated to be 76,012 design cycles. Assuming that the cyclic pressure condition spanning MAOP is typical, there is no reason to expect that a fatigue failure will occur within the life of the flowline. This statement is based on the fact that no cracks are present and that the anchor dent represents a blunt defect without any appreciable metal loss.

Figure 5 shows details of the analysis model including the geometry of the indenter and the boundary conditions applied to the finite element model. To achieve the maximum depth of 1.0 inches in the half-symmetry model, an indenter force of 209,770 lbs. was required. Once the indenter was removed, a residual dent depth of 0.786 inches remained in the pipe. It is thought that a total force of 419,540 lbs. was required to generate the dent in the actual pipe.

Figure 6 shows the residual von Mises stress state that is calculated after the removal of internal pressure (corresponds to Step # 7). As noted in this figure, the stress field in the vicinity of the dent exceeds the material yield strength of 70 ksi. This trend is also observed 90 degrees relative to the location of the dent on the side of the pipe. It is these latter stresses that are of primary concern when discussing the capacity of the pipeline to resist buckling due to external pressure.

In addition to addressing the effects of cyclic internal pressure on the fatigue life of the flowline, a limit analysis was also performed to determine the influence of the dent on the buckling capacity of the pipe. **Figure 7** shows the deflection of the dented pipe region as a function of external pressure. A limit analysis involves the application of increasing loads (in this case external pressure) to the point where gross disproportionate displacements occur. The load at which this occurs is defined as the lower bound collapse load. As shown in **Figure 7**, once a pressure of approximately 14,000 psi is reached, the displacement increases without bound, defining this pressure as the lower bound collapse load. The external pressure at the 7,700-ft water depth (shown as the **SOLID RED** line in this figure) is approximately 25 percent of the 14,000 psi pressure value, indicating that a safety margin of 4 exists relative to the external pressure at which buckling is likely to occur. In other words, it is unlikely that the flowline will buckle even in the event of complete internal pressure loss at a water depth of 7,700 feet.

DROPPED OBJECT STUDY USING LIMIT ANALYSIS

An analysis was performed to assess the potential damage associated with dropping a tie-in spool on an export riser. The objective was to determine the range of loads imparted to the riser and the corresponding damage due to a direct impact. To perform the assessment, limit analysis techniques were used based on finite element methods. The method involved quantifying the energy generated during a quasi-static denting process from an assumed drop height. One variable monitored and addressed in the analysis was the impact reaction load generated by the 16,000 lbs. dropped spool piece. Dropping the object from a relatively short height (less than 5 feet), the calculated reaction force was 660 kips, resulting in a 2-inch deep dent. Experimental work performed by the author confirms that an amplification of 40 g's is not unreasonable when considering impact force. Additionally, experimental work performed by Bharracharya, K.C., et al [2] confirms the validity of this observation.

The sections that follow provide details on the analysis methods and results associated with this study.

Analysis Methods

The primary purpose in performing the analysis of the dropped spool piece was to estimate the level of damage generated by impact with the active gas export riser. This effort involved using finite element methods to calculate the response of the gas line to the impact force generated by the dropped 16,000 lbs. spool piece. The following paragraphs provide background details on the analysis efforts and address the following three topics:

- Velocity of the dropped object at the time of impact
- Reaction force generated by the spool piece using energy methods
- Energy associated with the dropped object at impact

Calculating the Velocity of the Spool Piece at Impact

Prior to performing an assessment of the forces generated by the impact of the dropped spool piece, calculations were required to estimate the velocity at the point of contact with the export gas line. A schematic is provided in **Figure 8** showing the position of the spool piece above the surface of the water and the gas export line. As noted in this figure, the following heights are important in the velocity calculations:

- Height of the spool piece above the water surface: approximately 16 feet
- Height of the water surface above the export riser: approximately 57 feet

Figure 8 also shows the positions of interest during the projected path of the dropped spool piece. Position #1 is the initial position, Position

#2 corresponds to the water line (16.5 feet below the initial position of the spool piece), and Position #3 marks the location of export piping (57 feet below the water line). Calculating the velocity at any point during the fall involves assessing the potential energy, kinetic energy, and work associated with drag forces. The following equations were developed to address the changes in position during the fall. Variables of interest are:

m	Mass of the spool piece (lbm or slugs)
v	Velocity (ft/sec)
g	Acceleration of gravity (ft/sec ²)
h	Height (feet)
F _{drag}	Drag force associated with motion in water (lbf)

From Location #1 to Location #2 (conservation of energy):

$$\frac{1}{2}mv_1^2 + mgh_1 = \frac{1}{2}mv_2^2 + mgh_2$$

From Location #2 to Location #3 (conservation of energy including work due to drag force in water):

$$\frac{1}{2}mv_2^2 + mgh_2 = \frac{1}{2}mv_3^2 + mgh_3 + F_{drag} \cdot (h_2 - h_3)$$

The last term in the above expression corresponds to the work done by the drag force once the spool piece enters the water and moves to Position #3 (the point of impact). Drag force is defined using the following relation.

$$F_{drag} = \frac{1}{2}C_D \cdot \rho \cdot A \cdot v^2$$

where:

C _D	Drag coefficient associated with geometric profile (dimensionless, value of 0.35 assumed [3])
ρ	Density of water (slugs/ft ³)
A	Projected area of geometry (ft ²)

By combining the above set of equations, an expression is developed for calculating the velocity (v₃) at the point of impact with the export riser pipe.

$$v_3 = \sqrt{\frac{v_1^2 + 2g(h_1 - h_2) + 2g(h_2 - h_3)}{1 + \frac{C_D \cdot \rho \cdot A \cdot (h_2 - h_3)}{m}}}$$

Assuming an initial velocity, v₁, of zero, the velocity at the point of impact, v₃, is 40.8 feet per second:

$$v_3 = \sqrt{\frac{(0 \cdot \frac{ft}{sec})^2 + 2(32.2 \text{ ft/sec}^2)(73.5 \text{ ft})}{1 + \frac{0.35 \cdot 1.938 \frac{slugs}{ft^3} \cdot 23.3 \text{ ft}^2 \cdot (57 \text{ ft})}{489 \cdot slugs}}} = 40.8 \frac{ft}{sec}$$

As points of reference, the following velocities were also calculated.

- Free fall in air from 73.5 feet: v₃ = 68.8 ft/sec
- Free fall in air from 16.5 feet: v₂ = 32.6 ft/sec (velocity at point of impact with water)
- Free fall in water from 57 feet: v₃ = 35.9 ft/sec (assuming for v₂ an initial velocity of zero)

The terminal velocity of the spool piece in water is calculated to be 44.1 feet per second. This is the maximum velocity that can be achieved in water during a free fall of the spool piece and is calculated by setting the weight of the spool piece equal to the drag force in water (the drag force is a quadratic function of the velocity).

Once the velocities were calculated, analyses to assess impact loads were done. The impact loads determine the level of energy imparted to the gas export riser pipe from the dropped spool piece. **Table 1** lists the velocities as functions of position during the free fall of the spool piece. Using the calculated velocity at impact of 40.8 feet per second, the kinetic energy at impact for the 16,000 lbs spool piece is calculated to be 414 kip-ft (561 kJ). This study addresses the energy capacity of the export line and whether the energy associated with the dropped spool piece exceeded that energy capacity.

Damage Assessment Using Energy Methods

The methodology used to determine the level of impact damage done to the gas export riser started with calculating the level of energy required to create a 2-inch deep dent in the pipe. This value was selected by the author based on prior experience and recognizing that the 2-inch dent likely represented a lower bound value (i.e. actual damage associated with the dropped spool piece would have an energy far greater than that required for a 2-inch deep dent). The calculated result was the drop height required to produce this level of damage. A finite element model was constructed and analyzed using the ABAQUS Standard (version 6.4) general purpose finite element code. **Figure 9** shows the finite element model that includes the rigid surface geometry that was used to model the flange of the spool piece. Non-linear material properties with a bilinear stress-strain curve were used for the pipe along with non-linear strain-displacement relations. A half-symmetry model was used to reduce computational time of the analysis. The steps involved in the analysis were as follows:

Step #1: Apply internal design pressure of 3,000 psi to pipe

Step #2: Move indenter vertically down into pipe 2.00 inches

Step #3: Remove indenter to obtain residual dent (analysis resulted in a residual dent depth of 1.53 inches)

Step #4: Remove internal pressure

In terms of boundary conditions, the bottom nodes of the pipe were constrained in the vertical direction and the ends of the pipe were restrained axially. It could be argued that additional compliance can be achieved with boundary conditions having lower levels of restraint; however, the significant damage associated with the results of the analysis precluded the need for refining the boundary conditions. It was concluded that the damage was significant enough that there was no need to optimize the boundary conditions.

Figure 10 is a flow chart that shows the steps involved in the energy method analysis. As noted, the first objective was to plot the reaction force during denting as a function of displacement. Integrating the area under this curve calculates the work done during the denting process.

Figure 11 shows the load-displacement plot. It should be noted that this plot only shows the force required for creating an initial dent depth of 2 inches that which resulted in a residual dent depth of 1.53 inches.

Figure 12 shows the energy level during indentation as a function of dent depth. The energy was calculated by numerically integrating in a spreadsheet the load deflection data (area under the load-displacement curve shown in **Figure 11**). Also included on the right hand side of this plot are the estimated heights required to produce various indentation levels. The following conclusions are derived from the energy method model.

- Model calculates an initial indentation level of 2 inches using a quasi-static force
- A quasi-static force of 600,000 lbs is required to produce the assumed dent to the depth of 2 inches
- To produce the assumed dent, the 16 kip spool piece is dropped from approximately 4.5 feet in the air

Closing Comments

With increased activity in the Gulf of Mexico, coupled with the extensive cost and risk associated with dropped objects on subsea components, there has been significant interest in assessing the effects of dropped objects on the structural integrity of subsea systems. The study presented in this paper represents a relatively small-scale effort; however, the concepts and principles associated with the analysis methodology are consistent with what is done on larger dropped object studies. The core issue is to determine the energy capacity of a subsea system and whether or not a particular dropped object possesses sufficient energy to overcome the inherent capacity of that particular system. As confirmed in this study, the second-order relationship with velocity at impact is a primary contributor to impact energy.

The analysis results show that the export pipe has an energy capacity on the order of 70 kip-feet (95 kJ); however, the dropped spool piece possesses an impact a kinetic energy of 413 kip-ft (561 kJ). The obvious conclusion is that the spool piece poses a significant threat to the export line if it is dropped from the assumed height.

REPAIR OF RISERS USING COMPOSITE MATERIALS

Composite systems are a generally accepted method for repairing corroded and mechanically damaged onshore pipelines. The pipeline industry has arrived at this point after many years of research and investigation. Because the primary mode of loading for onshore pipelines is in the circumferential direction due to internal pressure, most composite systems have been designed and developed to provide hoop strength reinforcement. With advances in chemistry, several of the repair systems employ resins that cure underwater.

Although some composite repairs of offshore pipelines and risers have been done, there are legitimate concerns regarding the ability of these systems to provide adequate reinforcement in these environments. Unlike onshore pipelines, offshore pipes (especially risers) are subjected to significant tension and bending loads. As a result, there is a need to evaluate the current state of the art of using composite materials to repair offshore pipelines and risers. For this reason, a joint industry project was organized including three composite repair manufacturers. The intent of the effort was to determine the capability of composite materials to reinforce simulated corrosion in risers considering testing loads that included internal pressure, tension, and bending.

The primary intent of this test program was to evaluate the level of reinforcement provided to a corroded region of the riser pipe. In addition to tests performed on the repaired pipe sample, initial testing was also performed to determine strains in an unrepaired test sample that served as the base case to which all repaired results were compared.

The sections that follow include information on the test set-up and results for a carbon fiber based composite repair system developed by Comptek Structural Composites, Inc. (Comptek) of Boulder, Colorado.

Test Set-up

In this part of the study, experimental methods were used to assess the performance of composite materials in reinforcing risers. A limit load study was undertaken to assess the performance of simulated corrosion in a riser subjected to internal pressure (2880 psi held constant), tension (145 kips held constant), and bending loads. These loads were increased to the level needed to achieve significant plasticity in the corroded (repaired) region.

Sample preparation started by using an 8.625-inch x 0.403-inch, Grade X46 pipe and machining a simulated circumferential corrosion groove as shown in **Figure 13**. The wall thickness of the pipe was reduced by 50 percent over a length of 24 inches. Strain gages were installed on the sample before the installation of the repair as shown schematically in **Figure 14** and in a photograph, **Figure 15**. Weld caps were welded to the end of each test piece to impose the desired loading and retain the pressure.

Once the samples were prepared, Comptek installed the engineered repair system that used an epoxy resin with a combination of composite fabrics that included both carbon and E-glass. This system was specifically designed to reinforce the damage intentionally machined into the test samples. **Figure 16** shows the installation of this repair system.

Figure 17 shows a basic schematic of the test set-up with the instrumentation configuration. A total of 12 strain gages were installed including six mounted in the corroded steel region beneath the repair. Data were continuously monitored and then recorded at a rate of 1 scan per second. Strain gage readings were recorded, along with internal pressure, axial tension, and displacement, both horizontal and vertical. For the test sample loading, both axial tension and internal pressure were applied to the sample and held constant. Bending loads were then applied incrementally to the test sample up to the point where the collapse load was found.

Test Results

Strain gage data were post-processed after testing. **Figure 18** plots strain gage data for the repaired and unrepaired samples. In reviewing these data there are several noteworthy observations.

- Locations A and B are located beneath the composite repair. As shown for the strain data at both of these locations, the strain in the repaired region is significantly reduced when compared to the unrepaired data (RED line).
- It is noted for both Locations A and B that the strain in the pipe does not increase in proportion to the unrepaired sample beyond 40,000 lbs. Once plasticity begins in the steel, the composite material picks up the load and the local stiffness of the system increases. This is especially true for a carbon fiber system as it has a relatively high stiffness when compared to E-glass (4-5 times stiffer).
- Even at loads beyond the point where gross plasticity is induced in the undamaged section of pipe (Location C), the strain beneath the repair is limited to 0.20 percent. This is important from a design standpoint as a probable failure mode for corroded risers is elevated strain level in the steel.

Closing Comments

It is clear from the presented results, that the carbon fiber composite system provides a high level of reinforcement to the damaged riser pipe.

The benefit in using a limit load-based testing method is that it permits an assessment of strain in the damaged region that can then be compared to acceptable limits. As an example, if it is determined beforehand that the riser pipe can be subjected to 0.35 percent strain (provided here merely as an example), then the results presented herein indicate that with 50 percent corrosion the damaged region has been adequately reinforced for the short-term. What has not been presented or discussed in this paper are long-term degradation issues of the repair itself that must be considered. At the present time there is considerable research being done in this area that will shed new insights on this critical design criterion.

CONCLUSIONS

Analysis results for four unique engineering applications have been presented. Prior to advances made in the application of limit analysis using high speed computers, engineers were required to reduce complex structures to simplified geometries that would permit stability analysis using closed-form solutions. In the absence of more rigorous analysis methods such as those discussed in this paper, these simplifications were the only options that existed. The shortcomings of these approaches were that overly-conservative design criteria were required. These approaches resulted in the construction of heavy structures with unnecessarily high levels of stiffness, especially for repairs. Along the same lines, the limitations in terms of what engineers consider regarding structural stability and the mechanisms that could lead to instability and catastrophic failure have now improved.

The methods of limit load analyses and limit state design using both analytical and experimental techniques resolve many of the shortcomings associated with stability analysis based on classical methods. As shown in the four examples presented in this paper, limit state analyses permit the evaluation of structural stability for complicated structures including non-linearities for material properties and surface contact. The benefits are two-fold. First, engineers are able to evaluate and design complex structures in conjunction with more traditional design approaches based on stress and deformation criteria. Secondly, when performing limit analyses, engineers are better positioned to understand the potential failure mechanisms due to overload and are therefore able to establish design conditions to ensure the safe and reliable operation structures.

REFERENCES

- [1] Biel, R.C., and Alexander, C.R.; *Applications of Limit Load Analyses to Assess the Structural Integrity of Pressure Vessels* PVP2005-71724, ASME, Denver, CO, July 2005
- [2] Bharracharya, K.C., et al., *Impact Studies on Structural Components Using a Free-flight Drop Tower*, *Experimental Techniques*, pages 52 – 58, March/April 2006.
- [3] Fox, R. W., and McDonald, A. T., *Introduction to Fluid Mechanics* (Third Edition), John Wiley & Sons, New York, 1985, page 460.

ACKNOWLEDGEMENTS

The author would like to express his appreciation to Mr. Richard C. Biel, P.E. of Stress Engineering Services, Inc. for his review of this paper and insights on limit analysis methods. Additional, Mr. Jim Lockwood, P.E. and Dr. Larry Cercone of Comptek Structural Composites, Inc. contributed the use of their test data associated with the composite repair study.

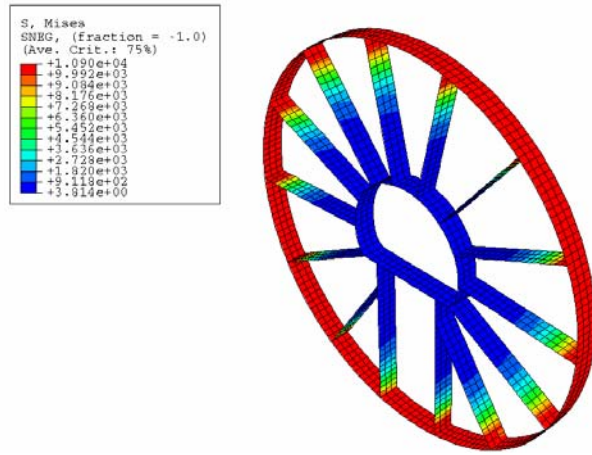


Figure 1 - Von Mises stress contour plot for finite element model

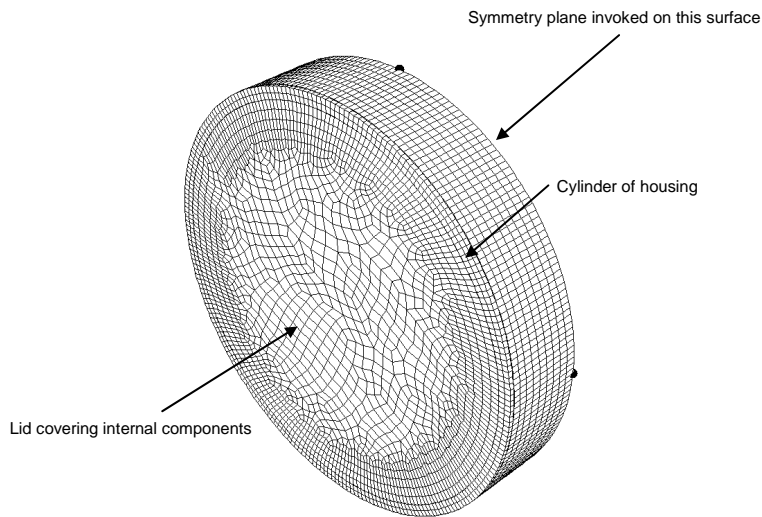


Figure 2 - Isometric view of solid finite element model

ABAQUS VERSION 6.3-5 DATE 21-SEP-2003 TIME 17:09:37

SUMMARY OF JOB INFORMATION:
 MONITOR NODE: 25752 DOF: 2

STEP	INC	ATT	TOTAL ITERS	TOTAL TIME/ FREQ	STEP TIME/LPF	INC OF TIME/LPF	DOF MONITOR
1	1	1	6	0.100	0.100	0.1000	-0.00267
1	2	1	5	0.200	0.200	0.1000	-0.00481
1	3	1	5	0.350	0.350	0.1500	-0.00782
1	4	1	5	0.575	0.575	0.2250	-0.0124
1	5	1	11	0.913	0.913	0.3375	-0.0241
1	6	2	6	0.934	0.934	0.02187	-0.0359
1	7	2	5	0.940	0.940	0.005469	-0.0469
1	8	3	4	0.941	0.941	0.001000	-0.0574

THE ANALYSIS HAS NOT BEEN COMPLETED

Figure 3 - ABAQUS status file output for finite element model

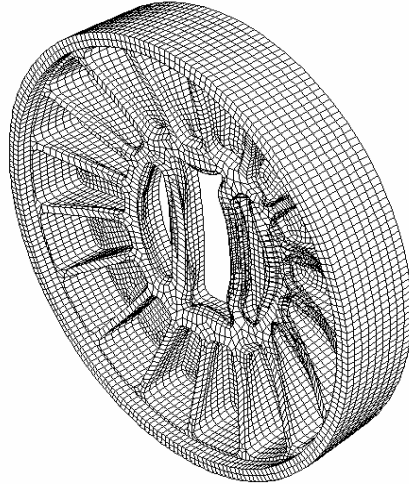


Figure 4 - Displaced shape for the solid finite element model (1X magnification)

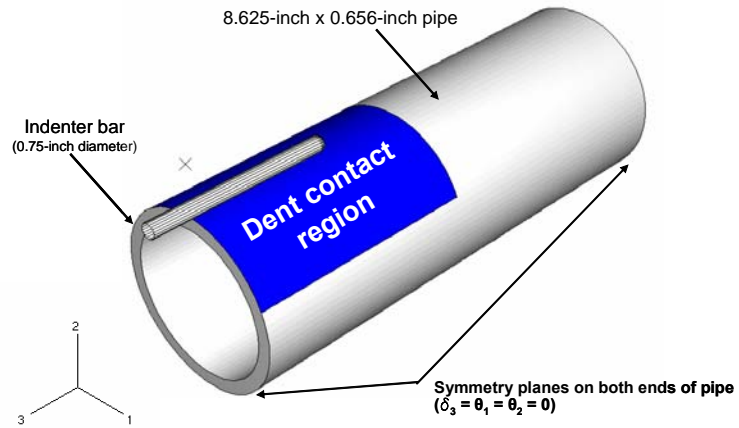


Figure 5 - Geometry for finite element model (half-symmetry geometry)

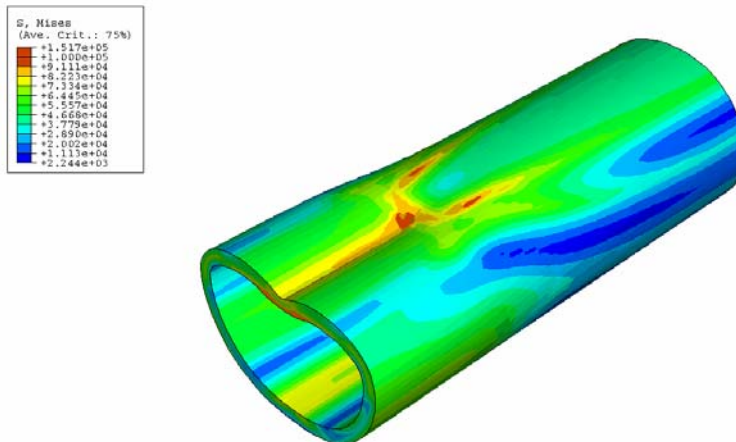


Figure 6 - Von Mises stress after internal pressure removed (residual stress state)
(Magnification factor on displacement of 2.4)

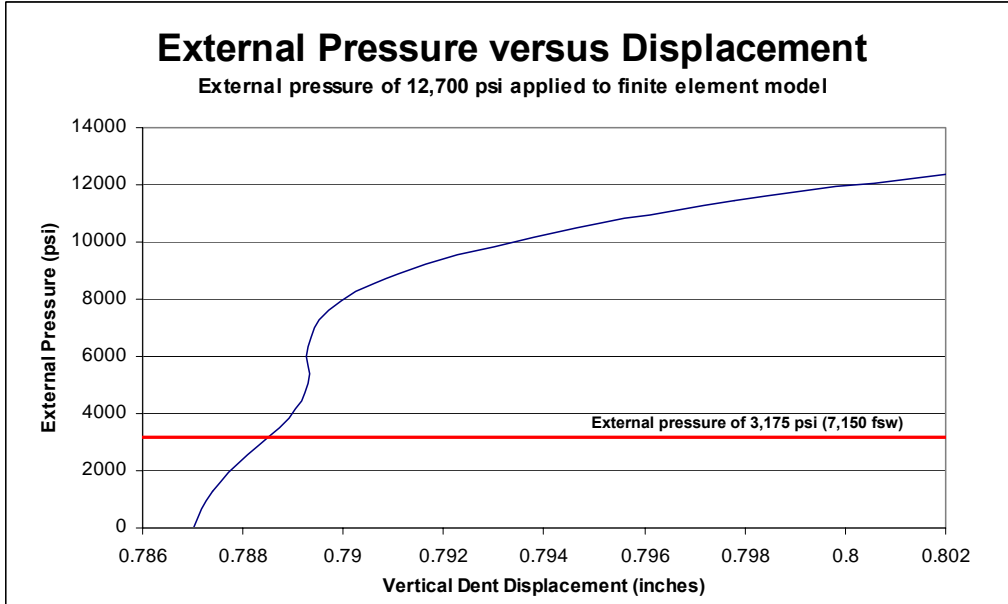


Figure 7 -Response of dented pipe to elevated external pressures

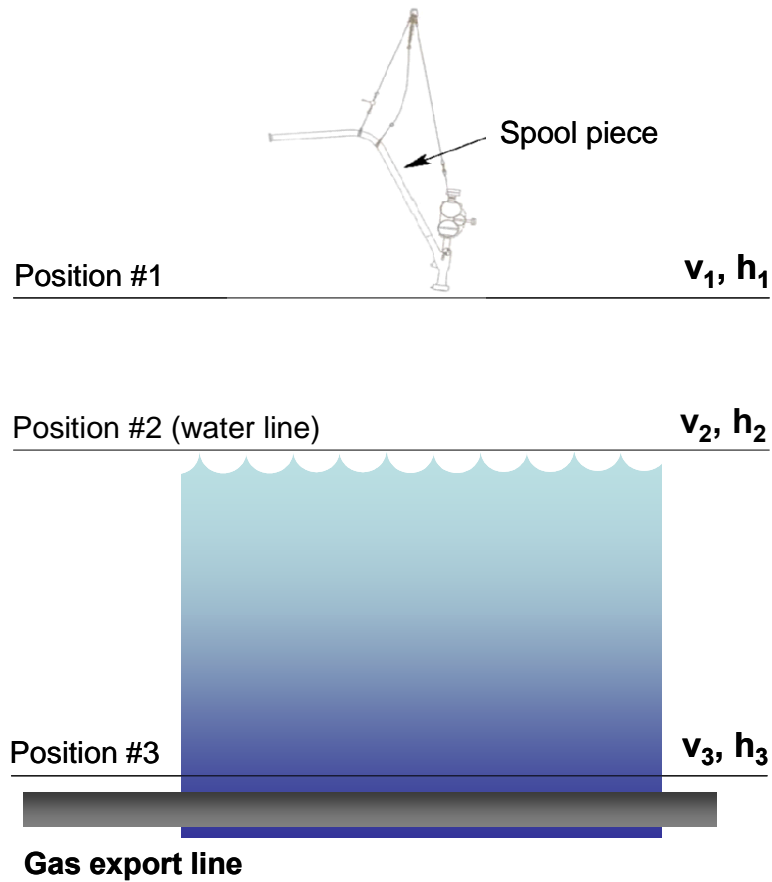


Figure 8 - Positions of interest associated with falling path of spool piece

Table 1 - Height and Calculated Velocity Values

Position	Height above export line (feet)	Velocity at position (ft/sec)
Position #1 (h_1 and v_1)	73.5	0 (initial value)
Position #2 (h_2 and v_2)	57	32.6 (impact with water)
Position #3 (h_3 and v_3)	0	40.8 (impact with pipe)

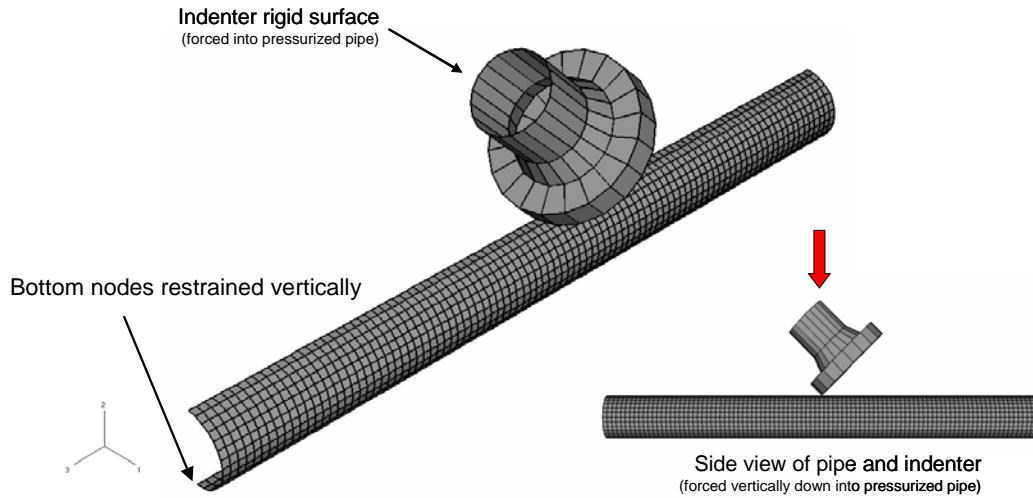


Figure 9 - Geometry of finite element model include rigid surface for spool flange

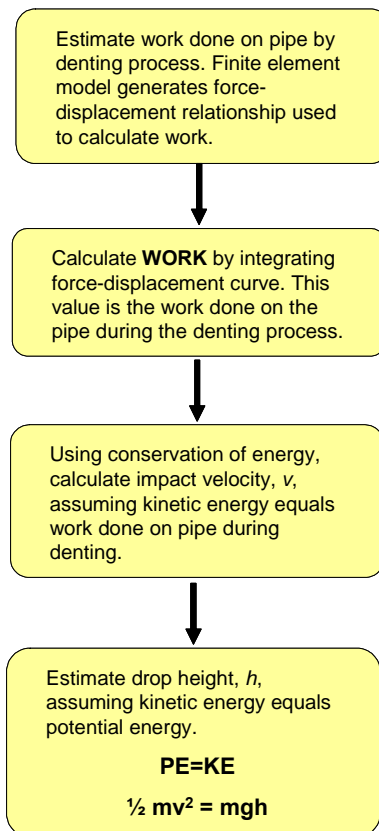


Figure 10 - Flow chart showing steps involved in energy method assessment

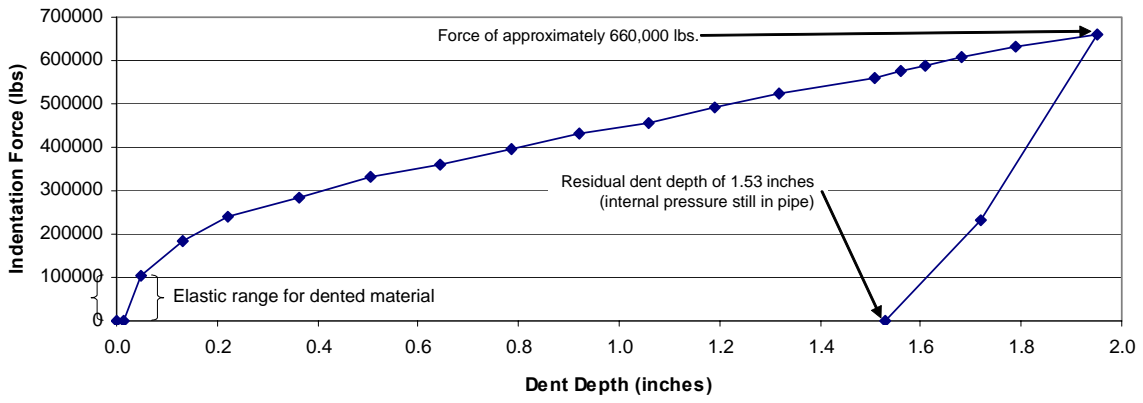


Figure 11 - Calculated force-displacement results

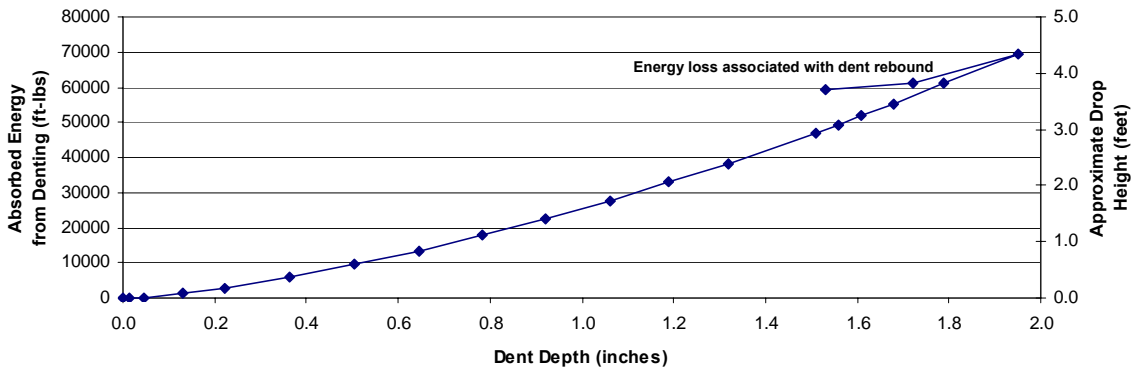


Figure 12 - Energy created during indentation as a function of dent depth (the above results are calculated by numerically integrating the data in Figure 11)

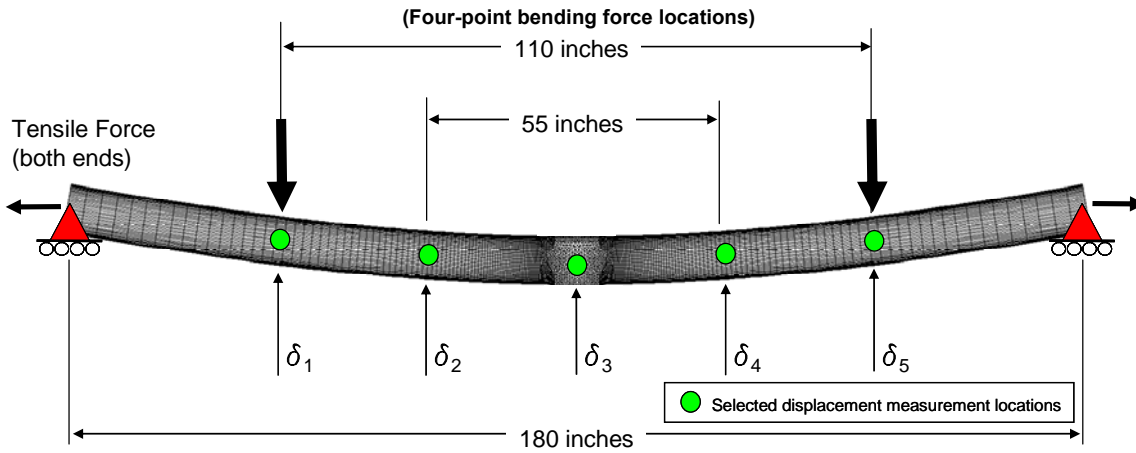


Figure 13 – Schematic diagram showing configuration of bend test sample

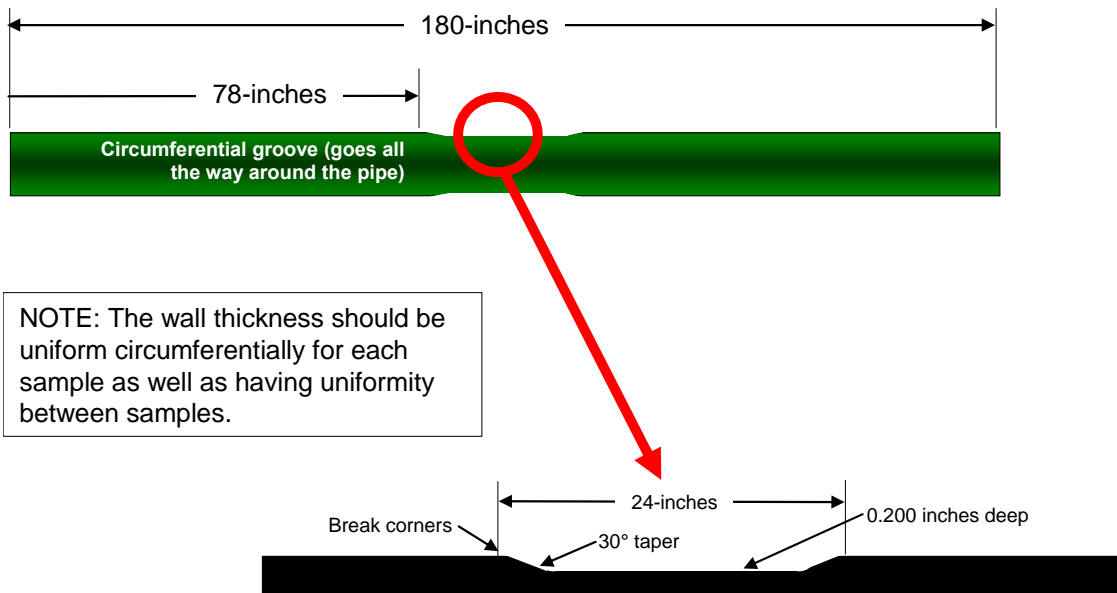


Figure 14 – Schematic diagram showing dimensions of simulated corroded region

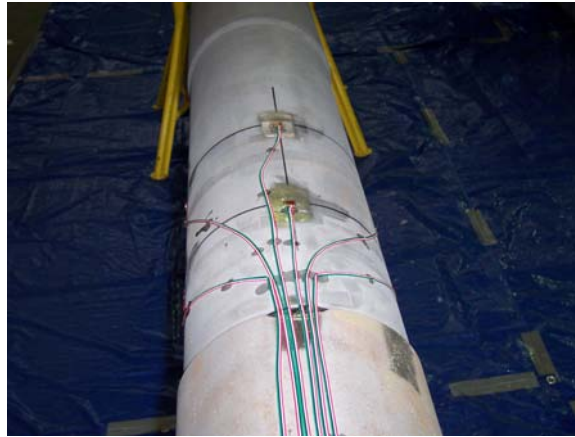


Figure 15 – Strain gages installed on test sample prior to installation of repair



Figure 16 – Installation of composite repair

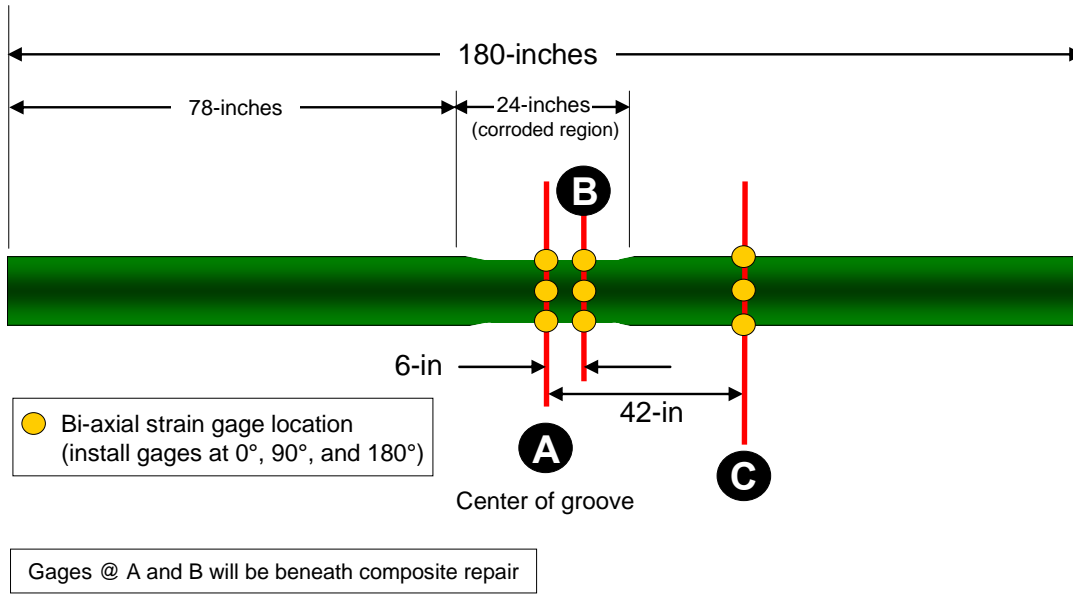


Figure 17 – Schematic diagram showing location of strain gages relative to defect zone

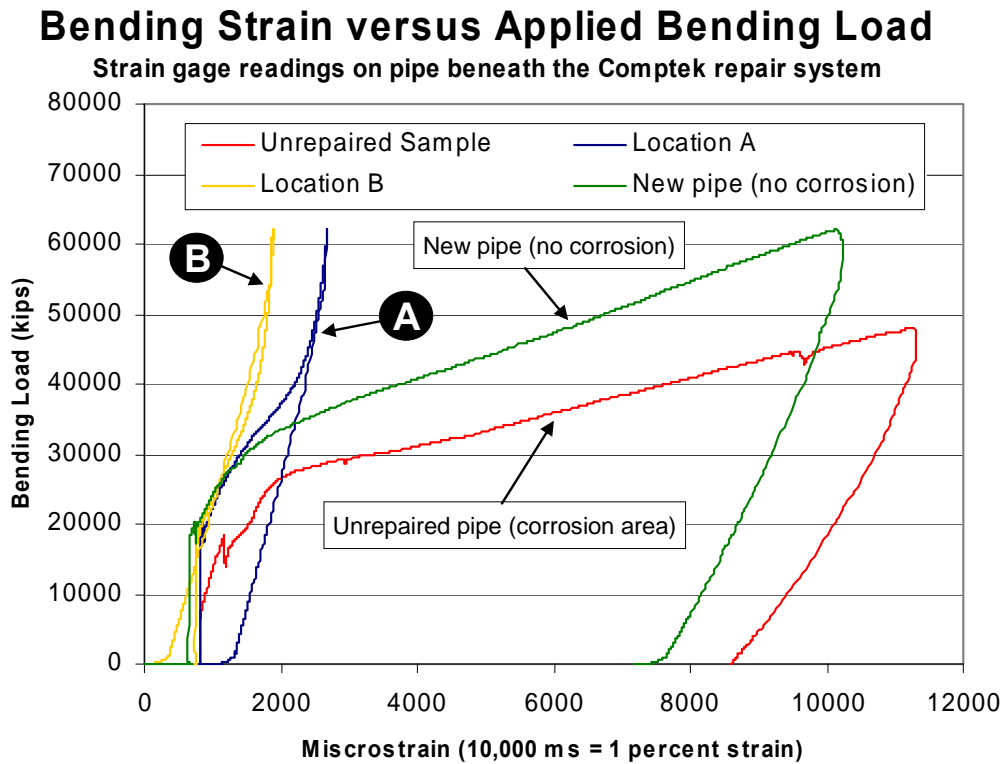


Figure 18 – Strain gage results acquired during bend testing of repaired corrosion sample